BRAF Mutations in Colorectal Cancer are Linked to Loss of *hMLH1* Expression and Proximal Location, while Independent of *KRAS* Activation.

Anna Colomer[1], Nadina Erill[1], August Vidal[1,2], Ruth Román[1], Montse Verdú[2], Carlos Cordon-Cardo[1,3], Xavier Puig[1,2].

[1]BIO**PAT**, Grup Assistència, Barcelona, Spain; [2]HISTOPAT Laboratoris, Barcelona, Spain; [3]Division of Molecular Pathology, Memorial Sloan-Kettering Cancer Center, New York.

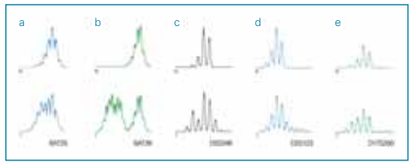

Figure 1

Electropherograms obtained from microsatellite instability testing using the five markers of the NCI panel. Representative appearance of a tumor exhibiting the MSI-H phenotype. For each marker, the top graph represents normal DNA and the bottom graph represents tumor DNA. (a) BAT25, (b) BAT26, (c) D5S346, (d) D2S123 and (e) D17S250.

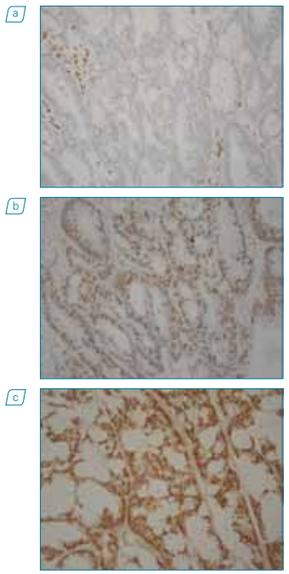

Figure 2

Representative examples of immunohistochemical stainings in colorectal cancers using monoclonal antibodies anti-MMR. (a) Lack of *hMLH1* expression in a MSI-H mucinous adenocarcinoma harboring the *BRAF*-V600E mutation (200x). (b) Normal *hMSH2* expression in the previous case (200x). (c) Normal *hMSH6* expression in a MSS mucinous adenocarcinoma carrying a G13D *KRAS* mutation (200x).

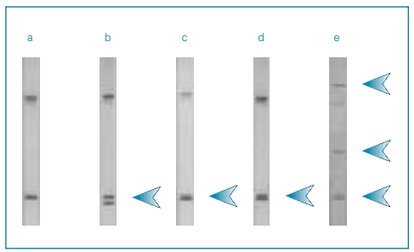

Figure 3

Exon 15 mobility profile of the *BRAF* gene analyzed by SSCP. Representative examples of the mobility shifts identified and subsequently confirmed as mutations by direct sequencing. (a) Wild type pattern. (b) D594G missense mutation. (c) G596R missense mutation. (d) V600E missense mutation. (e) Frame-shift mutation produced by a 2 bp deletion.

INTRODUCTION

BRAF is a member of the *RAF* gene family and encodes a cytoplasmic *RAS*-regulated serine/threonine kinase that mediates cellular responses to growth signals upstream of MEK1/2 kinases. Mutations within the *BRAF* gene occur in a number of human cancers, including malignant melanoma, thyroid cancer, and about 10% of colorectal carcinomas. *BRAF* mutations are significantly associated to DNA mismatch repair-deficient colorectal tumors due to gene silencing of *hMLH1* promoter by methylation. A single T to A transversion at nucleotide position 1796 resulting in a valine to glutamine substitution (V600E, previously V599E), accounts for most *BRAF*-activating point mutations. It leads to constitutive *ERK* activation, allowing evasion of apoptosis by induced survival. It has been reported that detection of the V600E mutation in colorectal tumors exhibiting microsatellite instability (MSI phenotype) argues against the presence of germline mutations in either the *hMLH1* or *hMSH2* gene, and could be used as a strategy for the detection of HNPCC families. Furthermore, *BRAF* and *KRAS* have been suggested as alternative genetic events in colorectal cancer, which reinforce the role of the *RAS/RAF/MEK/ERK* pathway in MSI-H carcinogenesis.

In this study, we investigated the incidence of *BRAF* mutations and its relationship with *KRAS* mutations and tumor location in a large consecutive series of primary colorectal cancers in regard to both microsatellite instability status and *hMLH1* gene expression.

PATIENTS AND TISSUES

Between February 1996 and June 2004, 267 consecutive tumor samples were collected prospectively from an equal number of patients surgically treated for colorectal cancer in the area of Barcelona, Spain. A final cohort of 244 patients was included in this study, since the remaining 23 cases (8.6%) were excluded due to poor DNA quality or deficient amplification. Demographic data on this cohort may be summarized as follows: 143 patients (59%) were males and 101 (41%) females; median age was 68.6±12.1 years (range 36-98). The table on the right summarizes data concerning clinicopathological features of the tumors.

Tissues included in the study were routinely fixed in 10% buffered formalin and embedded in paraffin. Representative hematoxylin and eosin-stained (H&E) sections of each case were examined microscopically by a pathologist, who selected viable representative areas of paired normal and tumor tissue for DNA extraction.

METHODS

Tissue Macrodissection, DNA Isolation and Quality Control.
Ten 5-µm-thick sections were used for each paired case (N and T samples) to perform manual scrapping. DNA was isolated using a proteinase K-phenol/chloroform protocol. Specific PCR reactions (200 ng of DNA per reaction) were performed once checked the quality of DNA by amplification of a 268 bp fragment of the human ß-globin gene.

Analysis of Microsatellite Instability.
Tumors were studied to assess their MSI status using eleven microsatellite markers. Five microsatellites from the NCI panel (BAT25, BAT26, D5S346, D2S123 and D17S250) were coamplified using the HNPCC Microsatellite Instability Test (Roche Molecular Biochemicals, Mannheim, Germany) according to manufacturer. Five microsatellites markers from a consensus panel originally aimed at elucidating the LOH status of chromosome 18q (D18S55, D18S58, D18S61, D18S64 and D18S69) were also amplified in multiplex reactions. An additional microsatellite aimed at looking at LOH at the TP53 locus on 17p (P53CA) was set up as a single reaction. Fluorescent amplicons were analyzed on an automated ABI® PRISM 310 Genetic Analyzer (Perkin Elmer Corporation, Norwalk, Conneticut) using the GeneScan software (PE Applied Biosystems, Foster City, CA).
Instability was assigned to a marker if its fragment pattern displayed either additional peaks or the appearance of separated novel fragments when the profiles of normal and tumor tissue were compared with each other. In accordance with consensus definitions of the US NCI, tumors were classified as exhibiting high microsatellite instability (MSI-H) when 30% or more of the tested loci resulted unstable, and non-MSI-H when they were less than 30%.

Immunohistochemistry for MMR Gene Expression.
Four-µm-thick sections were heated in citrate buffer for antigen retrieval. Pretreatment with avidin and biotin was also required for blocking endogenous biotin prior to incubation with the primary monoclonal antibodies, that were anti-hMLH1 (clone G168-15), anti-hMSH2 (clone G219-1129), and anti-hMSH6 (clone 44), all purchased from BD Biosciences Pharmingen, San Diego, CA. Secondary antibody was a biotinylated horse anti-mouse (Vector Laboratories Inc., Burlingame, CA). Detection was performed using the avidin-biotin complex Vectastain Elite ABC PK 6100 (Vector Laboratories), the peroxidase reaction was developed using diaminobenzidine tetrachloride as chromogen, and Harris-modified hematoxylin was used as nuclear counterstain. Positive controls were tumors known to have positive nuclear staining. The corresponding negative controls –in which the primary antibody was omitted– were included in each experiment.

Lack of protein expression was recorded when none of the tumor nuclei stained for *hMLH1*, *hMSH2* or *hMSH6*, being cases reported as hMLH1–, hMSH2–, or hMSH6–, respectively. Positive staining of nuclei in intact adjacent crypt bases and lymphocytes served as an internal control. Tumors with intact expression in any tumor nuclei were recorded to have normal protein expression.

Mutational Analyses of BRAF and KRAS.
Amplicons of 313 and 224 bp in size were obtained from single PCR reactions that spanned the entire exon 11 and the exon 15 of the *BRAF* gene, respectively. Mutational analysis of the exon 15 was performed by SSCP in GeneGel Excel 12.5/24 polyacrylamide non-denaturing pre-cast gels (Amersham Pharmacia Biotech, Uppsala, Sweden) that were developed by silver staining. Samples showing mobility shifts were retest by bidirectional sequencing of a new exon 15 amplicon –prepared with a fresh template of the tumor sample– using the ABI PRISM® BigDye® Terminator v1.1 Cycle Sequencing Kit (Applied Biosystems, Warrington, UK). Exon 11 was directly approached by bidirectional sequencing with the same kit cited above.

An amplicon of 107 bp in size was obtained by PCR that encompassed codons 12 and 13 of the *KRAS* gene. Mutational analysis was also performed by direct sequencing using an internal reverse primer.

Statistical Analyses.
BRAF mutations were investigated for their association with MSI status, *MMR* gene expression, and the presence of *KRAS* mutations by Fisher's exact test of contingency tables with odd ratio calculation (OR) as appropriate. *p*-values were considered statistically significant when less than 0.05. Data were analyzed using the R package v.2.0.0 (2004-04-10) (©2004, R Development Core Team).

RESULTS

The table on the right summarizes data used for statistical analyses.

Twenty-five out of 244 cases (10%) exhibited the MSI-H phenotype (Figure 1). Within this group, 19 tumors were found to lack expression of *MMR* genes and, of those, 18 cases were hMLH1–, whereas one case was hMSH2– (Figure 2). As expected, the lack of *hMLH1* expression was found to be associated with the MSI-H phenotype (Fisher's exact test, $p<0.001$), since only one case out of 219 exhibiting the MSS phenotype was reported as hMLH1– (OR= 0.0020 [0.0001-0.0155]).

Fourteen tumors out of the 19 that exhibited the MSI-H phenotype lacking expression of *MMR* genes (74%) harbored a *BRAF* mutation at exon 15 by SSCP –latter confirmed as V600E by sequencing–, in the absence of *KRAS* mutations. Of the 5 tumors within this group lacking *BRAF* mutations, one was a MSH2–, while 2 lesions carried *KRAS* mutations, and 2 cases were suspected HNPCC based on the early age of onset (48 and 55 years old). None of these cases had mutations in exon 11 of the *BRAF* gene. In agreement with other reports, *BRAF* mutations were found to be related to *hMHL1* expression (Fisher's exact test, $p<0.001$), being more common in hMLH1– tumors than in those keeping normal expression (OR= 34.97 [10.35-140.47]).

Twenty cases out of 219 that exhibited the MSS phenotype (9%) displayed mobility shifts at exon 15 of the *BRAF* gene (Figure 3). Sequencing analyses revealed that 14 tumors of the 15 sharing a common SSCP pattern harbored the V600E whereas the one left had a G596R mutation, 3 had a D594G, and the last had a 2 base-pair deletion at codon 599 that produced a premature stop codon (Figure 4). No *KRAS* mutation was detected at any lesion harboring a *BRAF* mutation, which suggests that both alterations are mutually exclusive events (Fisher's exact test, $p<0.001$).

Regarding tumor location, the V600E tended to occur in proximal rather than in distal tumors (Fisher's exact test; $p<0.001$; OR= 9.66 [3.61-30.40]), and especially significant is the fact that all mutations detected in MSI-H tumors belonged to proximal lesions.

CONCLUSIONS

These results support the hypothesis that *BRAF* and *KRAS* mutations are mutually exclusive events associated with sporadic MSI-H colorectal cancer lacking *hMLH1* expression.

More studies should be performed in order to clarify the role of the *RAS/RAF/MEK/ERK* pathway in colorectal carcinogenesis, since *BRAF* is a candidate therapeutic target which could provide novel strategies for clinical management of MSI-H colorectal cancer.

REFERENCES

- Davies H, Bignell GR, Cox C, et al. Mutations of the *BRAF* gene in human cancer. *Nature* 2002;417:949-54.
- Deng G, Bell I, Crawley S, et al. *BRAF* mutation is frequently present in sporadic colorectal cancer with methylated *hMLH1*, but not in hereditary nonpolyposis colorectal cancer. *Clin Cancer Res* 2004;10:191-5.
- Domingo E, Espin E, Armengol M, et al. Activated *BRAF* targets proximal colon tumors with mismatch repair deficiency and MLH1 inactivation. *Genes Chromosomes Cancer* 2004;39:138-42.
- Domingo E, Laiho P, Ollikainen M, et al. *BRAF* screening as a low-cost effective strategy for simplifying HNPCC genetic testing. *J Med Genet* 2004;41:664-8.
- McGivern A, Wynter CV, Whitehall VL, et al. Promoter hypermethylation frequency and *BRAF* mutations distinguish hereditary non-polyposis colon cancer from sporadic MSI-H colon cancer. *Fam Cancer* 2004;3:101-7.
- Miyaki M, Iijima T, Yamaguchi T, et al. Both *BRAF* and *KRAS* mutations are rare in colorectal carcinomas from patients with hereditary nonpolyposis colorectal cancer. *Cancer Lett* 2004;211:105-9.
- Rajagopalan H, Bardelli A, Lengauer C, et al. Tumorigenesis: RAF/RAS oncogenes and mismatch-repair status. *Nature* 2002;418:934.

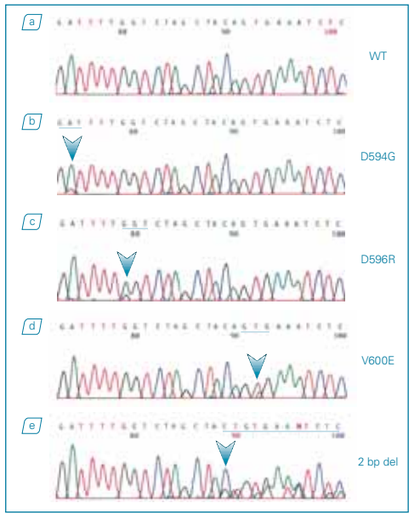

Figure 4

Representative examples of *BRAF* mutations identified by sequencing analysis in colorectal cancers. (a) Wild type sequence. (b) A to G change at codon 594 that resulted in a missense mutation Asp to Gly. (c) G to C change at codon 596 that resulted in a missense mutation Gly to Arg. (d) T to A change at codon 600 that resulted in a missense mutation Val to Glu. (e) CA deletion at codon 599 that resulted in a frame-shift mutation creating a premature stop codon within the exon.

Table

Tumor features (n = 244)	MSI-H (n = 25)	Non-MSI-H (n = 219)
Location		
Proximal	20 (80.0)	64 (29.2)
Distal	5 (20.0)	146 (66.7)
Not specified	0 (0.0)	9 (4.1)
Tumor type [A]		
Adenocarcinoma	14 (56.0)	197 (90.0)
Mucinous adenocarcinoma	10 (40.0)	22 (10.0)
Undifferentiated carcinoma	1 (4.0)	0 (0.0)
Histologic grade [B]		
1	6 (24.0)	97 (44.7)
2	3 (12.0)	86 (39.6)
3 or 4	16 (64.0)	34 (15.7)
Extent of invasion [C]		
pT1	2 (8.0)	15 (6.9)
pT2	4 (16.0)	29 (13.2)
pT3	14 (56.0)	102 (46.6)
pT4	5 (20.0)	73 (33.3)
Stage [D]		
A	5 (20.0)	36 (16.5)
B	12 (48.0)	64 (29.2)
C	8 (32.0)	97 (44.3)
D	0 (0.0)	22 (10.0)
MMR expression		
Normal	6 (24.0)	218 (99.5)
hMLH1–	18 (72.0)	1 (0.5)
hMSH2–	1 (4.0)	0 (0.0)
hMSH6–	0 (0.0)	0 (0.0)
KRAS mutation		
Absent	21 (84.0)	121 (55.2)
Present	4 (16.0)	95 (43.4)
Not valuable	0 (0.0)	3 (1.4)
BRAF mutation		
Absent	10 (40.0)	197 (90.0)
Present	15 (60.0)	20 (9.1)
Not valuable	0 (0.0)	2 (0.9)

A Histologic type was assigned according to the WHO classification.
B Grade was assigned according to the WHO classification that considers mucinous adenocarcinomas and undifferentiated carcinomas as Grade 3 and 4, respectively. Two preoperatively radiated lesions were ungradeable.
C Extent of tumor invasion was assigned according to the TNM (UICC) system.
D Clinical stage was based on the Astler-Coller's modification of the Dukes system.